Journal of Hazardous Materials 496 (2025) 139356

Contents lists available at ScienceDirect

Journal of Hazardous Materials

journal homepage: www.elsevier.com/locate/jhazmat

Complex combined effects of polystyrene nanoplastics and phenanthrene in aquatic models

Paloma De Oro-Carretero [a,*,1], Marlid Garcia-Ordoñez [b,1], Nerea Roher [b,c,d], Jon Sanz-Landaluze [a]

[a] Department of Analytical Chemistry, Faculty of Chemical Science, Universidad Complutense de Madrid, Avenida Complutense s/n, Madrid 28040, Spain
[b] Institute of Biotechnology and Biomedicine, Universitat Autònoma de Barcelona, Barcelona 08193, Spain
[c] Department of Cell Biology, Animal Physiology and Immunology, Universitat Autònoma de Barcelona, Barcelona 08193, Spain
[d] Bioengineering, Biomaterials and Nanomedicine (CIBER-BBN), Spain

HIGHLIGHTS

- Co-exposure to PHE and PS-NPs resulted in lower toxicity compared to individual exposure in zebrafish larvae.
- Higher metabolites concentrations were observed in hepatocytes when PS-NPs were present in the medium.
- Cell and tissue type-dependent uptake of PS-NPs upon co-exposure with PHE.
- The presence of PS-NPs may induce synergistic or antagonistic effects.
- Effects may be influenced by agglomeration state and free PHE availability.

GRAPHICAL ABSTRACT

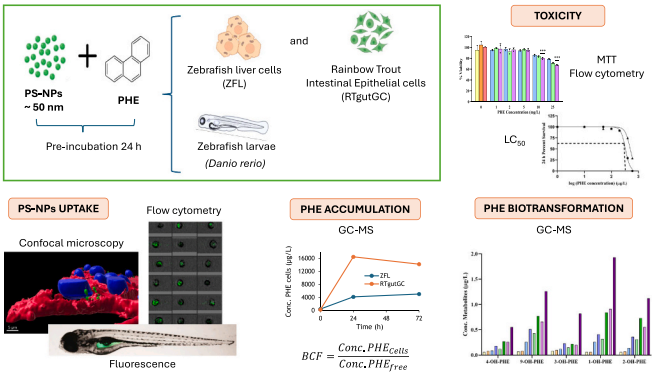

ARTICLE INFO

Keywords:
Nanoplastics
Phenanthrene
Co-exposure
Zebrafish larvae
Cells
Effects

ABSTRACT

Nanoplastic (NPs) pollution is an increasing social concern due to their potential to accumulate in aquatic environments and their ability to penetrate organisms. In addition, they can adsorb toxic chemicals from their surroundings and help to transfer them to organisms. This study evaluated the effects of co-exposure of polystyrene (PS)-NPs and phenanthrene (PHE) on toxicity, accumulation, and metabolization in two fish cell lines (zebrafish liver cells and rainbow trout intestinal cells) and in zebrafish. The uptake of PS-NPs was studied by cytometry and confocal microscopy while PHE uptake and metabolization was determined by extraction and detection of the compound and its major metabolites (hydroxy-phenanthrene, OH-PHEs) by gas chromatography coupled to mass spectrometry. Lower uptake of PS-NPs was observed in intestinal cells and zebrafish larvae gut in the presence of PHE, but higher uptakes were observed in zebrafish liver cells. Higher concentrations of PHE and its metabolites were detected in the presence of PS-NPs. Interestingly, zebrafish larvae experienced lower toxicity during co-exposure compared to single exposure. These results indicate that the interaction between PS-NPs and

* Corresponding author.
E-mail addresses: pdeoro@ucm.es (P. De Oro-Carretero), marlid.garcia@uab.cat (M. Garcia-Ordoñez), nerea.roher@uab.cat (N. Roher), jsanzlan@ucm.es (J. Sanz-Landaluze).
[1] Both authors equally contributed.

https://doi.org/10.1016/j.jhazmat.2025.139356
Received 21 February 2025; Received in revised form 22 July 2025; Accepted 23 July 2025
Available online 24 July 2025

PHE presents a synergistic effect with significant complexity, showing cell-type and tissue dependent ecotoxicological effects and suggesting differential pathways of uptake and distribution of these pollutants.

1. Introduction

In recent decades, the abusive production [1], use and release of plastics into the environment has become a social, scientific and political problem due to the huge environmental and public health consequences [2]. Plastic residues in both micrometric (diameter less than 5 mm – MPs) and nanometric size (less than 100 nm – NPs; [3], have been found in remote sites such as the Antarctica [4], rural waters and forest landscapes [5], food and beverages [6], as well as inside organisms and aquatic ecosystems [7]. Among all types of plastics, polystyrene (PS) is one of the most widely used polymers in different manufactured products [8]. With an intermediate density of 0.96–1.05 g/cm^3, close to that of the water, it is distributed in both surface and bottom waters, making it more bioavailable to aquatic organisms [9,10].

Concentrations of micro(nano) plastics (MNPs) in aquatic environments are directly correlated with human density and human activity [1]. According to Jambeck *et al.* [11], the largest contribution of plastic into aquatic environments originates from Asian countries (8.82 million metric tons/year), well above European countries (0.31 million metric tonnes/year). The highest concentration of MPs according to the study of Patidar *et al.* [12] in Asia was 372 ± 14.3 items·L^{-1} and 9630 ± 2947 items·kg^{-1} in water and sediments, respectively. In beach sediments from South Africa, 340.7–4757 items·m^{-2} were found [1]. In general, most studies have shown higher densities of MNPs on the seabed in coastal areas, with concentrations reaching up to 7700 items·km^{-2}. This is followed by floating marine litter at over 600 items·km^{-2} and, finally, beaches with a rate of 1 item/m^2 [13]. Although reliable quantification methods for NPs are still scarce, it is estimated that their concentration could be much higher than that of MPs [14]. Previous studies have detected PS-NPs in the range of 0.02–10^6 items·m^{-3} in aquatic environments [15]. Gallego-Urrea *et al.* [16] measured 10^7-10^9 particles·mL^{-1} by nanoparticle tracking analysis (NTA) in Scandinavian waters. In other aquatic environments such as Alpine snow [17] and the Atlantic Ocean [18], among others, PS-NPs were quantified in a range of 10^{-9}-10^{-4} g·mL^{-1} (10^6-10^{11} particles·mL^{-1} for 100 nm particles) [19].

MNPs may cause adverse effects on organisms and human health [20,21], because they easily penetrate biological membranes [22] and accumulate inside organisms [23]. However, MNPs are not isolated in the environment and, due to their high surface area/volume ratio and hydrophobicity, they can easily adsorb other pollutants, such as persistent organic pollutants (POPs) [24], facilitating their transport and internalisation in different living organisms (Trojan horse effect) [25]. Nanoplastics (NPs) have a much higher specific surface area, having a higher potential to penetrate biological membranes and to transport organic pollutants compared to MPs [26]. Polycyclic aromatic hydrocarbons (PAHs) are ubiquitous in aquatic environments [14], and they are adsorbed onto polystyrene MNPs by hydrophobic and π–π interactions [27]. These interactions depend on the planar surface and spatial arrangement and number of aromatic rings composing the structure of PAHs [28]. In phenanthrene, π-π stacking interactions are usually slightly predominant, due to its three linear and planar aromatic rings, unlike naphthalene [29] or benzo(a)pyrene [30], where hydrophobic or combined interactions predominate, respectively.

The toxicity of PAHs has been extensively studied and includes oxidative stress, endocrine disruption, carcinogenicity and genotoxicity [31,32]. Phenanthrene (PHE), is one of the most common PAHs found inside marine organisms [33] and is often used as a model for studying uptake and metabolism of small PAHs [34]. The range of PHE concentrations reported by Peng *et al.* [35] in aquatic environments was between 153 ng·L^{-1} and 1460 μg·L^{-1}. Wu *et al.* [36] reported that PHE exposure concentrations in freshwaters in China range from 45.01 to 379.28 μg·L^{-1} and Miura *et al.* [37] found concentrations of 125–375 pg·m^{-3} PHE in the Pacific Ocean.

Most studies indicate that pollutant toxicity increases when combined with MNPs, with particular emphasis on pollutant uptake. However, few studies analyse how MNPs, interact with environmental pollutants and affect ecosystems and organisms beyond their general toxicity. Invertebrate models such as Daphnia (*D. magna* and *D. pulex*) and vertebrate models such as zebrafish, are commonly used to study the ecotoxicological effects of MNPs in the aquatic environment [20,38]. This work aims to investigate the interaction between polystyrene nanoplastics (PS-NPs) and PHE, to gain a better understanding of their impact on biological systems, specifically on the uptake and metabolic processes that occur when both substances coexist. In this regard, two *in vitro* models, each representing cells with different biological and functional backgrounds (i.e. zebrafish liver cells; ZFL, and rainbow trout intestinal cells; RTgutGC), were used. Each one representative of a cell type relevant for absorption (gut cells) and detoxification (liver cells).

In addition, to further understand the interaction and metabolisms of PHE and PS-NP combination *in vivo* we used zebrafish (*Danio rerio*) larvae. The absorption of PS-NPs was studied by fluorescence techniques, whereas PHE uptake and metabolization was determined by extraction and detection of the compound and its major metabolites (hydroxy-phenanthrene, OH-PHEs) by gas chromatography coupled to mass spectrometry.

2. Materials and methods

2.1. Nanoplastics and chemicals

Fluorescently labelled PS-NPs (42 nm - ref. FSDG001 Dragon Green) and non-labelled PS-NPs (44 nm - ref. PS02002) were purchased from Bang Laboratories (Fisher, IN, USA). PS-NPs were provided as a 1 % (w/w) suspension in water with 2 mM NaN_3. The characterization of NPs in different conditions (pure water, PBS, cell culture medium and embryo medium) was performed in a previous study [23]. Individual solid standard of PHE, fluorene (FLU), 1-OH-PHE, 2-OH-PHE, 3-OH-PHE, 4-OH-PHE and 9-OH-PHE were supplied by Sigma Aldrich (Madrid, Spain).

2.2. Preparation of PS-NPs solutions with sorbed PHE (NPs-PHE)

PS-NPs and PHE dilutions were prepared by mixing the corresponding volumes of PS-NPs in PBS and PHE in methanol (MetOH, Scharlab) and then further diluted in culture medium (Dulbecco's modified Eagle's medium [DMEM] for ZFL and Leibovitz medium L-15 for RTgutGC; see Section 2.3) or E3 medium (see Section 2.8) for zebrafish larvae, to obtain the final concentrations in the experiments. The concentration of methanol present in each solution was less than 1 % for all conditions studied. For flow cytometry and confocal microscopy fluorescent PS-NPs were used. For MTT (3-(4,5-dimethylthiazol-2-yl)-2,5-diphenyltetrazolium bromide, Sigma-Aldrich) viability assays and PHE absorption and metabolization assays, non-fluorescent PS-NPs were used. All solutions were carried out in sealed glass vials and subsequently incubated for 24 h in the dark at 25 ºC with horizontal rotary shaking (120 rpm).

Table 1 shows the solutions prepared for the different experiments, listing the individual concentrations of PS-NPs and PHE used both independently and in their combined exposure. Concentrations of PS-NPs were selected in a way that did not cause toxicity on individual exposures according to previous studies [17,31], (i.e. 10, 25 and 50 mg·L^{-1} PS-NPs; 1–5·10^{11} particles·mL^{-1}). These levels are within or

close to the range of concentrations reported in the environment, such as those previously reported, thereby ensuring environmental relevance despite ongoing challenges in detecting and quantifying nanoplastics *in situ*. Sendra et al. [40] used 10 mg·L^{-1} PS-NPs as environmentally relevant concentration in surface water and in agreement with other ecotoxicological studies with NPs in aquatic organisms. Regarding PHE, the concentrations applied in our assays (resulting in freely dissolved concentrations between 0.12 and 0.79 mg·L^{-1}; see Table 2 and Supplementary Information) remain below its aqueous solubility limit (0.82 mg·L^{-1}; 4.6 μM [41]) and were selected to ensure surface saturation of PS-NPs [26,42]. Importantly, these PHE exposure levels are consistent with concentrations found in natural aquatic environments, which range from 45.01 to 379.28 μg·L^{-1} in freshwaters in China [36] and up to 1460 μg·L^{-1} as reported by Peng *et al.* [35]. While some experimental concentrations approach the upper end of environmental values, they remain within ecologically realistic scenarios, especially in polluted or urban-impacted environments, which are increasingly relevant for assessing combined pollutant effects.

2.3. Cell culture

ZFL cells (CRL-2643, American Type Culture Collection, ATCC) were cultured at 28°C, in humidified air atmosphere and 5 % CO_2 in Dulbecco's modified Eagle's medium (DMEM; 4.5 g·L^{-1} glucose, supplemented with 10 % (v/v) heat-inactivated fetal bovine serum (FBS), 5 % (v/v) antibiotic/antimycotic solution, 0.01 mg·mL^{-1} insulin, 50 ng·mL^{-1} Epidermal Growth Factor (EGF) and 0.5 % (v/v) heat inactivated trout serum (TS), as described in Torrealba *et al.* [43]. RTgutGC cells (obtained from Dr. C. Tafalla's laboratory) were cultured at 20°C in Leibovitz's L-15 Medium GlutaMAX™ without CO_2, supplemented with heat-inactivated FBS 10 % (v/v) and 1 % antibiotic/antimycotic [44]. Subconfluent cultures were detached by adding TrypLE Express (Gibco) for 5 min. All experiments were performed with phenol red-free culture media to avoid any potential phenol red interference [45,46].

2.4. PHE + PS-NPs cytotoxicity studies in ZFL and RTgutGC cells

The toxicity of PHE in the presence of PS-NPs was assessed using the MTT assay. ZFL and RTgutGC cells were incubated with 2, 5, 10, 25 and 50 mg·L^{-1} and 1, 2, 5, 10, and 25 mg·L^{-1} of PHE, respectively, and in combination with 10 mg·L^{-1} and 50 mg·L^{-1} of PS-NPs (Table 1, solutions prepared according to Section 2.2). Cells were incubated for 24 and 72 h, then washed with PBS and the MTT (Sigma-Aldrich) was added at 10 % of the total volume at a final concentration of 0.5 mg·mL^{-1} and incubated for 30 min. After incubation, the MTT solution was removed, the formazan crystals were dissolved in dimethylsulfoxide (DMSO) and the absorbance quantified at 550 nm on a Victor3 Plate Reader (PerkinElmer). Data were normalized to control readings set at 100 %. A one-way ANOVA was performed comparing treatment and control means using Prism software (GraphPad). Three independent assays were carried out using the same conditions.

In addition, cell viability in ZFL cells was tested with BD Via-Probe™ Red Nucleic Acid Stain by flow cytometry. For this, cells were subjected to similar conditions as those in the MTT trial and subsequently detached with TrypLE Express (Gibco) and sedimented by centrifugation at 300 ×g for 5 min. Cell pellets were resuspended in PBS and 0.5 μL of BD Via-Probe™ Red reagent (5 μM) was added. A total of 10000 events were recorded by flow cytometry (CytoFLEX Beckman Coulter, Inc.) and data analysed using Flowing Software 2.5.1 (University of Turku, Finland).

2.5. Uptake of PS-NPs in the presence of PHE. Cytometry and confocal microscopy

The uptake of fluorescent PS-NPs at 10 and 50 mg·L^{-1} (non-toxic concentrations) was assessed in ZFL cells under different concentrations of phenanthrene (0, 2, 5, 10, 25 and 50 mg·L^{-1}) during 24 and 72 h (Table 1). PS-NPs-PHE solutions were prepared according to Section 2.2. After treatment, cells were detached with TrypLE Express during 5 min and cells were retrieved by centrifugation at 300 x *g* for 5 min. Pellets were resuspended in PBS for flow cytometry (FACSDiscover S8 Cell Sorter with CellView, BD), and 10,000 events were counted. In addition to the uptake and Mean Fluorescence Intensity (MFI), the imaging technology of the cell sorter was used to analyse some conditions (50 mg·L^{-1} PS-NPs vs 50 mg·L^{-1} PS-NPs + 25 mg·L^{-1} PHE). In the same way, internalization was measured in RTgutGC cells at 25 mg·L^{-1} PS-NPs in combination with 0, 10 and 25 mg·L^{-1} PHE to observe differences in the response of enterocytes after 72 h of exposure. Previous study reported higher internalisation rates in RTgutGC compared to ZFL, thus lower PS-NPs concentrations (i.e. 25 mg·L^{1}) were selected to avoid saturation of the control image [39].

To confirm that the fluorescence observed by cytometry was due to the PS-NPs accumulated inside the ZFL cells and not merely attached to the cell membrane surface, confocal microscopy (Zeiss LSM 700) was performed. ZFL cells were seeded on 35 mm ibidi glass-bottom plates and when 60 % confluence was reached, cells were treated with 25 mg·L^{-1} PS-NPs and 25 mg·L^{-1} PS-NPs + 25 mg·L^{-1} PHE for 24 h. Cells were stained with Hoechst (nuclei) and Cell Mask Deep Red (membrane) (Life Technologies). Images were analysed with Imaris v9.3 (Bitplane) and ImageJ (National Institute of Health, USA) software.

2.6. Bioaccumulation and metabolization of PHE: cell and medium extraction and determination by GC-MS

Methodologies for exposure, extraction, derivatization, separation, and detection, previously developed and validated [47,48] were employed in the current study for ZFL and RTgutGC cell lines. In the case of RTgutGC cells, although a formal method optimization has not been

Table 1
Experimental details of PS-NPs and PHE concentrations and study times for each experiment performed.

Evaluation	Organism	Determination	PS-NPs Fluorescent Label	Conc. PS-NPs (mg·L^{-1})	Conc. PHE (mg·L^{-1})	Exposure time
Toxicity	ZFL	MTT	No	0, 10 and 50	0, 2, 5, 10, 25 and 50	24 and 72 h
	RTgutGC	MTT	No	0, 10 and 50	0, 1, 2, 5, 10 and 25	24 and 72 h
	ZF larvae	Dose-response	No	0 and 5	0, 0.001, 0.01, 0.05, 0.1, 0.2, 0.4 and 0.6	24 h
Uptake of PS-NPs	ZFL	Flow cytometry	Yes	0, 10 and 50	0, 2, 5, 10, 25 and 50	24 and 72 h
		Confocal microscopy	Yes	0 and 25	0 and 25	24 h
	RTgutGC	Flow cytometry	Yes	0, 10 and 25	0, 10 and 25	72 h
	ZF larvae	Fluorescence image	Yes	0 and 5	0 and 0.05	48 h
Bioaccumulation and biotransformation of PHE	ZFL	GC-MS	No	0, 10 and 50	0, 10, 25 and 50	0, 24 and 72 h
	RTgutGC	GC-MS	No	0, 10 and 50	0, 10 and 25	0, 24 and 72 h
	ZF larvae	GC-MS	Yes	0 and 5	0, 0.01, 0.05 and 0.1	24 h

Table 2
Medium (C_{med}) and cell (C_{cell}) concentration determined experimentally and free concentration (C_{free}) estimated by MBM.

Cell line	ZFL				RTgutGC			
Treatment conditions	**C_{med} ($mg \cdot L^{-1}$)**	**C_{free} ($mg \cdot L^{-1}$)**	**C_{cell} ($mg \cdot kg^{-1}$)**	**BCF ($L \cdot kg^{-1}$)**	**C_{med} ($mg \cdot L^{-1}$)**	**C_{free} ($mg \cdot L^{-1}$)**	**C_{cell} ($mg \cdot kg^{-1}$)**	**BCF ($L \cdot kg^{-1}$)**
10 mg/L PHE (0 h)	11	0.18	-	-	15	0.28	-	-
10 mg/L PHE (24 h)	6	0.09	6	59	9	0.16	2	15
10 mg/L PHE (72 h)	9	0.15	7	49	8	0.15	3	18
10 mg/L PHE + 10 mg/L PS-NPs (0 h)	11	0.19	-	-	14	0.25	-	-
10 mg/L PHE + 10 mg/L PS-NPs (24 h)	7	0.12	4	34	10	0.17	16	82
10 mg/L PHE + 10 mg/L PS-NPs (72 h)	9	0.15	5	33	11	0.20	14	72
10 mg/L PHE + 50 mg/L PS-NPs (0 h)	11	0.19	-	-	13	0.24		
10 mg/L PHE + 50 mg/L PS-NPs (24 h)	8	0.14	5	38	10	0.18	7	37
10 mg/L PHE + 50 mg/L PS-NPs (72 h)	13	0.22	6	26	11	0.20	9	44
25 mg/L PHE (0 h)	25	0.43	-	-	29	0.53	-	-
25 mg/L PHE (24 h)	12	0.20	29	141	13	0.23	6	26
25 mg/L PHE (72 h)	11	0.19	27	146	12	0.22	4	17
25 mg/L PHE + 10 mg/L PS-NPs (0 h)	23	0.38	-	-	24	0.44	-	-
25 mg/L PHE + 10 mg/L PS-NPs (24 h)	17	0.29	32	111	20	0.36	45	126
25 mg/L PHE + 10 mg/L PS-NPs (72 h)	14	0.24	27	113	16	0.30	41	138
25 mg/L PHE + 50 mg/L PS-NPs (0 h)	27	0.46	-	-	28	0.51	-	-
25 mg/L PHE + 50 mg/L PS-NPs (24 h)	16	0.28	37	133	24	0.44	64	145
25 mg/L PHE + 50 mg/L PS-NPs (72 h)	14	0.24	24	101	23	0.43	72	169
50 mg/L PHE (0 h)	46	0.78	-	-				
50 mg/L PHE (24 h)	19	0.33	139	423				
50 mg/L PHE (72 h)	18	0.31	118	378				
50 mg/L PHE + 10 mg/L PS-NPs (0 h)	47	0.79	-	-				
50 mg/L PHE + 10 mg/L PS-NPs (24 h)	20	0.34	223	665				
50 mg/L PHE + 10 mg/L PS-NPs (72 h)	18	0.30	162	532				
50 mg/L PHE + 50 mg/L PS-NPs (0 h)	48	0.75	-	-				
50 mg/L PHE + 50 mg/L PS-NPs (24 h)	28	0.47	386	826				
50 mg/L PHE + 50 mg/L PS-NPs (72 h)	21	0.36	150	722				

published, extraction procedures followed the same protocol, and spiked samples were included in each extraction batch to assess recovery, which yielded consistently high recovery rates. ZFL and RTgutGC cells were treated with 10, 25 and 50 $mg \cdot L^{-1}$ PHE and 10 and 25 $mg \cdot L^{-1}$ PHE, respectively, in combination with 10 and 50 $mg \cdot L^{-1}$ PS-NPs (Table 1). After 24 and 72 h, the cell media and the cell pellets were collected including initial medium (0 h). For the determination of PHE and its metabolites, the cell pellets were divided into 2 fractions, dried under nitrogen stream and weighted. All samples were stored at −20 ºC until analysis.

For PHE quantification, half of the obtained pellets (~10 mg for ZFL cells and ~5 mg for RTgutGC cells) were extracted with 500 µL of hexane and sonicated with an ultrasound probe (Vibra cell VCx130, 2 mm diameter titanium microtip, 130 W high frequency generator at 20 KHz from Sonics & Materials Inc. USA), for 1 min at 30 % amplitude and an on/off:2 s/5 s pulse. For medium extraction (500 µL) a liquid-liquid extraction was performed with 500 µL of hexane and vortexed for 1 min. The extraction mixture was centrifuged for 10 min at 13,000 x g and the organic extract was measured by gas chromatography (Agilent Technologies Mod. 7890 A Series) coupled to mass spectrometry (HP 5975 C VL MSD) (GC-MS). Internal standard (fluorene, FLU) was previously added to the extraction step. Samples (1 µL) were injected in splitless mode at 280 ºC with Helium at a constant pressure of 25 psi. The temperature of the column (ZB-5 capillary column 30 m × 0.25 mm I.D., 0.25-µm film thickness) was programmed to increase from 90 ºC (1 min) to 250 ºC (1 min) at a rate of 70 $ºC \cdot min^{-1}$ and then to 270 ºC (1 min) at 40 $ºC \cdot min^{-1}$. The temperature of the ion source and the transfer line of the mass spectrometer was set at 250 and 270 ºC, respectively, and 70 eV for the electron beam. The other half of the pellet obtained and 500 µL of medium was used for OH-PHEs (1-OH, 2-OH, 3-OH, 4-OH and 9-OH-PHE) quantification.

Finally, after quantification of the total PHE concentration in the medium (C_{med}), the bioavailable concentration (C_{free}) was determined using mass balance models (MBM) to relate it to the concentration inside the cells (C_{cell}) and thus to estimate the bioconcentration factor (BCF) at each exposure time ($BCF_{24\ h}$, $BCF_{72\ h}$). Data analysis for C_{free} and BCF determination is described in the supplementary information as developed in De Oro and Sanz 2024 [48].

2.7. Zebrafish husbandry and breeding

Wild-type zebrafish (*Danio rerio*) were housed in a recirculating aquarium system and maintained at 28 ± 1 °C with a 12-hour light:dark photoperiod. Adult fish were fed twice daily with 2 % body weight. Ammonia, nitrite, pH, and nitrate levels were monitored daily. Ammonia was kept below detectable limits; nitrate concentrations did not exceed 100 $mg \cdot L^{-1}$ and the pH was maintained between 6.8 and 7.5. For breeding, one female and three males were placed in a breeding tank in the late afternoon, and embryos were collected the following morning. Fertilized eggs were collected, extensively washed with water and placed in petri dishes in E3 medium. Unfertilized and dead embryos were separated from viable ones with a plastic pipette (Deltalab). All zebrafish experiments complied with the International Guiding Principles for Research Involving Animals (EU 2010/63) and received prior approval from the Ethics Committee of the Universitat Autònoma de Barcelona (UAB, CEEH number 1582).

2.8. PHE and PHE + PS-NPs toxicity in Zebrafish larvae

Zebrafish larvae were exposed to different nominal concentrations of PHE in the presence or absence of PS-NPs. Control animals were incubated in E3 medium (5 mM NaCl, 0.17 mM KCl, 0.33 mM $CaCl_2$, 0.33 mM $MgSO_4$ and 0.1 % methylene blue) and the percentage of MetOH used as vehicle. Groups of 24 larvae (n = 48 per condition) were distributed on 96-well plates (Thermo Fisher) with one larvae per well containing 200 µl E3 medium or PS-NPs at 5 $mg \cdot L^{-1}$; alone, or in combination with PHE at concentrations of 1, 10, 50, 100, 200, 400 and 600 $\mu g \cdot L^{-1}$, pre-incubated for 24 h (Table 1). Mortality data was recorded 24 h post-treatment and analysed with GraphPad software with a logistic dose-response model to fit the data and to estimate the LC_{50} value.

2.9. Uptake of PS-NPs in presence of PHE in Zebrafish Larvae

Groups of four larvae (72 h post fertilization, hpf) per treatment were distributed on 96-well plates (Thermo Fisher) and immersed in 200 µL of E3 medium with PHE (50 µg·L^{-1}) and PS-NPs (5 mg·L^{-1}) (Table 1). Biodistribution in zebrafish larvae was evaluated after 48 h using a fluorescence stereomicroscope (Nikon SMZ800) coupled with a camera (Nikon DS-Fi2). Fluorescence was quantified using ImageJ software 1.53 t and expressed as Mean Fluorescence Intensity (MFI) normalized by the larvae area. The experiments were repeated 3 times (n = 12).

2.10. Bioaccumulation of PHE in presence of PS-NPs in Zebrafish Larvae

Groups of 9–12 larvae, depending on hatching and survival, were exposed to 10, 50 and 100 µg·L^{-1} PHE in combination with 5 mg·L^{-1} PS-NPs, respectively, for 24 h (Table 1). Larvae of each condition were then washed with fresh medium and stored in the same vial at −20 °C until analysis. The methodology and analytical equipment used for the determination of PHE inside larvae was the same as that used in Section 2.6 except for the ultrasound probe (1 min at 40 % amplitude and an on/off:1 s/s pulse, [49]).

2.11. Statistical analysis

Analysis of variance (ANOVA) was performed using Prism 8.01 software (GraphPad Prism) to assess significant differences among the results. A 95 % confidence level was applied in all analyses; thus, differences were considered statistically significant when the p-value was less than 0.05.

3. Results

3.1. PHE toxicity in the presence of PS-NPs in ZFL and RTgutGC cells

Analysis of viability using the MTT assay revealed that ZFL cells remained viable under all experimental conditions and doses of PS-NPs and PHE (Fig. 1), while no significant changes in viability were observed in cells only exposed to PS-NPs (10 mg·L^{-1} and 50 mg·L^{-1}) or MetOH (Fig. 1a and b). However, a decrease in viability was observed in ZFL cells exposed to 50 mg·L^{-1} PHE + 10 and 50 mg·L^{-1} PS-NPs for 72 h, with cell viability dropping to 78 % and 69 % (Fig. 1b), although these differences remained below the threshold for significance. Similarly, when we used Vita-Probe staining to assess viability by flow cytometry, no significant differences were observed in ZFL cells exposed to either PHE or PS-NPs. But as for MMT results, ZFL cells exposed to 50 mg·L^{-1} PHE + 50 mg·L^{-1} PS-NPs exhibited a significant decrease in viability down to 75 % at 24 h and 71 % at 72 h (Figure S1).

On the other hand, a more pronounced decrease in RTgutGC cell viability was observed in the MTT assay after 72 h of combined exposure to either 10 or 25 mg·L^{-1} PHE + 50 mg·L^{-1} PS-NPs, with viability

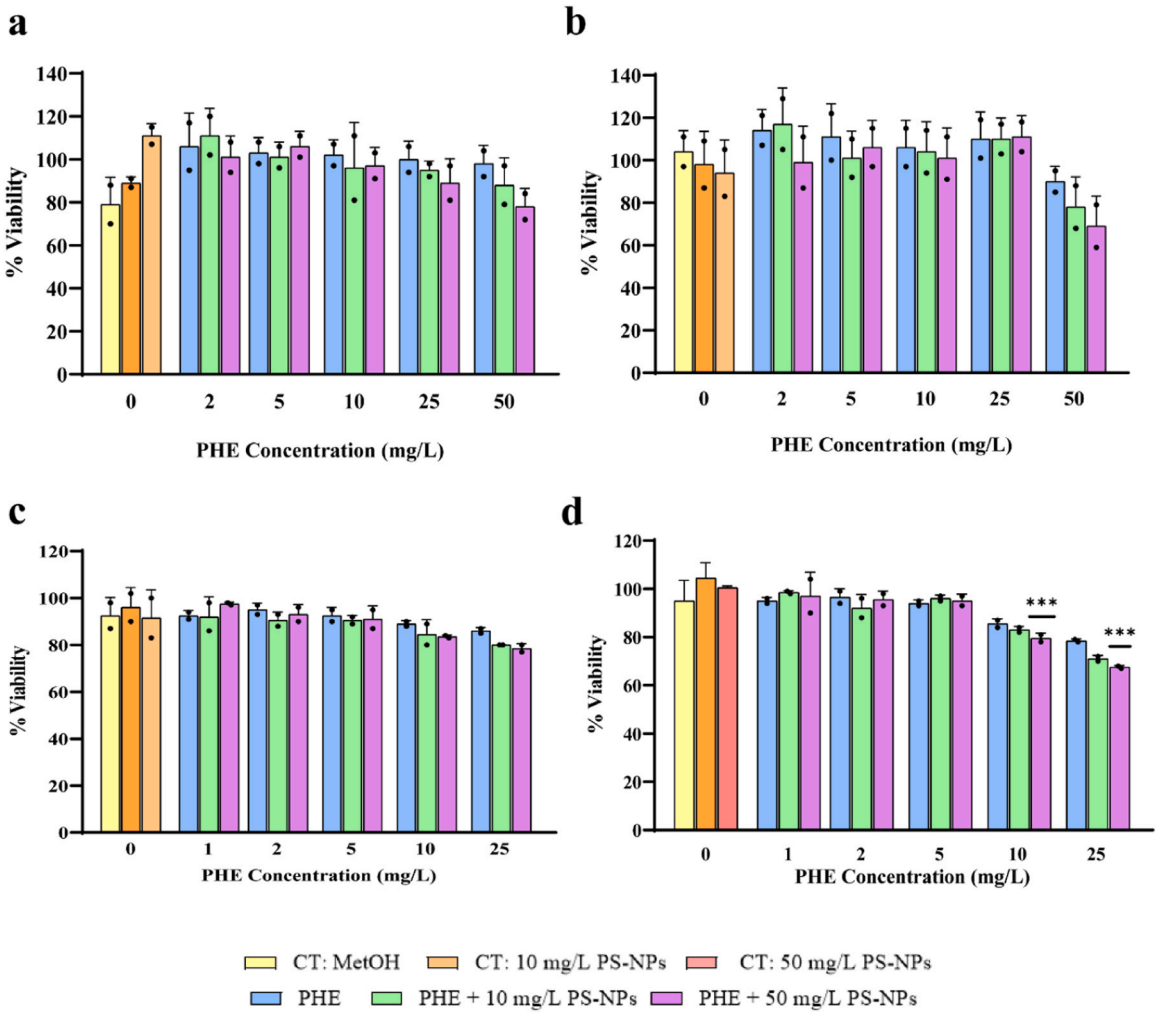

Fig. 1. Cell viability of ZFL and RTgutGC cells when exposed to PHE or PHE + PS-NPs (10 mg·L^{-1} and 50 mg·L^{-1}). a) ZFL cells for 24 h, b) ZFL cells for 72 h, c) RTgutGC cells for 24 h and d) RTgutGC cells for 72 h. Significance levels *p < 0.05.

significantly dropping to 80 and 71 %, respectively (Fig. 1c and d). Again, no significant changes in viability were observed in the cells only exposed to PS-NPs (10 mg·L^{-1} and 50 mg·L^{-1}) or MetOH (Fig. 1c and d).

3.2. Uptake of PS-NPs in ZFL and RTgutGC cells in the presence of PHE

The uptake of PS-NPs in the presence of different concentrations of PHE in two different cell types was evaluated by flow cytometry. We observed an increase in the percentage of fluorescent cells from 16.0 % to 53.5 % in ZFL cells exposed to 10 and 50 mg·L^{-1} PS-NPs at 24 h (Fig. 2a). When the cells were exposed to PS-NPs + PHE (25 mg·L^{-1}), a strong increase in the percentage of fluorescent cells and the total fluorescent signal intensity (MFI) was observed (Fig. 2a). Furthermore, as shown in Figure S2, it was observed that the percentage of fluorescent cells increased progressively with rising concentrations of PHE at both 24 h and 72 h after exposure to 50 mg·L^{-1} PS-NPs. However, in the case of 10 mg·L^{-1} PS-NPs, the percentage of fluorescent cells was constant (1–5 %) until exposure to 10 mg·L^{-1} PHE, with a subsequent significant increase after exposure to higher concentrations of PHE (25 and 50 mg·L^{-1}), reaching percentages of 15 and 75 % ($p = 0.0019$) at 24 h and 79 ($p < 0.0001$) and 89 % ($p < 0.0001$) at 72 h. Therefore, for the following experiments we decided to test 10, 25, and 50 mg·L^{-1} PHE. Uptake was also confirmed by flow cytometry imaging (Fig. 2b) and confocal microscopy (Fig. 2c), along with the internalization of PS-NPs in the presence of PHE (Fig. 2d). In contrast, as reflected by the values in Fig. 2e and confirmed by flow cytometry imaging in Fig. 2 f, RTgutGC cells show a higher percentage of fluorescent cells (70–80 %) than ZFL cells at both 10 and 25 mg·L^{-1} PS-NPs. Moreover, as the concentration of PHE in the medium increased, the MFI decreased (Fig. 2e).

3.3. Bioaccumulation and metabolization of PHE in ZFL and RTgutGC cells in presence of PS-NPs

The PHE concentrations inside ZFL and RTgutGC cells (C_{cell}) and in their culture media (C_{med}) at the different exposure scenarios and times (24 h and 72 h) are shown in Table 2. Bioavailable free concentration (C_{free}) was determined from C_{med} by MBM as explained in supporting information and BCF (C_{cell}/C_{free}) was estimated at each exposure time and condition (Table 2). As for internal PHE uptake, both hepatocytes and enterocytes show a rapid stabilization of PHE concentration, reaching constant values at 24 and 72 h in almost all conditions (Figure S3). In addition, hepatocytes exhibited a higher tendency to internalize and bioaccumulate PHE compared to intestinal cells when exposed solely to PHE. In contrast, when PHE was combined with PS-NPs, higher concentrations and BCF values were observed in RTgutGC cells compared to ZFL cells. When examining the cell lines separately, an increase in PHE uptake and bioaccumulation was observed in RTgutGC cells when exposed in combination with PS-NPs, compared to PHE alone. In ZFL cells, similar or even lower values of uptake and BCF were observed when PHE was combined with PS-NPs. Fig. 3 shows the concentrations of the main PHE metabolites (1-OH, 2-OH, 3-OH, 4-OH and 9-OH-PHE) found in ZFL cells at 10 mg·L^{-1} of PHE, showing that concentration of these metabolites increased over the exposure time. In addition, higher concentrations of PHE metabolites were detected when higher concentrations of PS-NPs were present in the medium. The same trend was observed in the experiments at 25 and 50 mg·L^{-1} PHE (Figure S4). In contrast, no metabolites were detected in RTgutGC cells.

3.4. PHE and PHE + PS-NPs toxicity in zebrafish larvae

We evaluate whether the presence of PS-NPs may modify the toxicity of PHE *in vivo* using zebrafish larvae. Groups of 48 larvae were incubated with PHE at different concentrations in the absence and presence of PS-NPs. From the experimental data, we estimated the LC_{50} of PHE to be 331.8 μg·L^{-1} while that of PHE with PS-NPs was 489.9 μg·L^{-1} (Fig. 4). The LC_{50} values were determined by plotting the 24 h survival percentage against the logarithm of PHE concentrations using GraphPad Prism. A non-linear regression analysis was performed using a sigmoidal dose-response (variable slope) model to fit the data and calculate the LC_{50}, which corresponds to the concentration of PHE that causes 50 % mortality in the zebrafish larvae.

3.5. Uptake of PS-NPs by zebrafish larvae in the presence of PHE

Representative images of PS-NPs uptake in larvae incubated 48 h with PS-NPs or PS-NPs combined with PHE in E3 medium are shown in Fig. 5a. The fluorescent PS-NPs accumulate in the digestive tract (Fig. 5a) both in the presence or absence of PHE. However, the MFI accumulated in the zebrafish larvae in the presence of PHE was significantly lower ($p = 0.0402$) (Fig. 5b).

3.6. Uptake of PHE in zebrafish Larvae in presence of PS-NPs

Fig. 5c shows the PHE concentrations inside the larvae (C_{larvae}) and the BCF (L·kg^{-1}) estimated as the ratio of C_{larvae} to the PHE nominal concentration of the different exposure scenarios. The concentrations were normalized according to the number of larvae and the weight of a larvae (0.44 mg, [49]). For all PHE concentrations studied, higher PHE concentrations were observed inside the larvae when exposed in combination with PS-NPs. However, this difference was not statistically significant.

4. Discussion

Many studies have demonstrated the synergistic toxicity of micro- and nanoplastics (MNPs) with organic compounds such as phenanthrene in different organisms [14,32,50]. On the other hand, other studies have reported the 'Trojan horse effect' [51] where MNPs act as entry vectors for organic compounds attached to their surface. In this study, we combined discussions of the results on toxicity, absorption and metabolization of PS-NPs and PHE to further explain the observed effects in fish cells lines with different functional backgrounds (liver cells and gut cells) and in living zebrafish larvae.

4.1. Cell and tissue type-dependent effects on PS-NPs and PHE co-exposure

The toxicity results in ZFL and RTgutGC cells indicated an increase in toxicity when PS-NPs and PHE were combined (Fig. 1). Katsumiti *et al.* [52] exposed *Mytilus galloprovincialis* hemocytes to 50 nm PS-NPs (10^2–10^{12} particles·mL^{-1}) and benzo(a)pyrene (BaP, 250 μg·L^{-1}) and reported that PAH alone had a higher toxicity (50 %) compared to the mixture, but this was observed at lower PS-NPs concentrations (ranging from 10^{11}-10^{12} particles·mL^{-1}) than in this study. At a concentration of 10^{12} particles·mL^{-1}, the mixture showed slightly higher toxicity (10 %) than individual compounds. Wang *et al.* [32] reported a 5–10 % increase in the mortality of hematocytes (*Mytilus coruscus)* when exposed to a mixture of NPs (30 μg·L^{-1} and 70 nm) and PHE (5, 50 and 500 μg·L^{-1}) compared to the exposure without NPs. Sun *et al.* [50] found that cell viability of coelomocytes of the earthworm *Eisenia fetida* under combined exposure to higher concentrations of BaP (150 μg·L^{-1}) and PS-NPs (7.5 mg·L^{-1} and 100 nm) was lower than that under single exposure, but not very significant (81 % of viability, compared to 82 % of only PS-NPs or 85 % of BaP). In general, a slight increase (no more than 10 %) in the toxicity of mixtures of NPs and PAHs is observed, especially at high concentrations of NPs consistent with the data from our experiments. Notably, the combined effects were either additive or antagonistic, suggesting that MNPs do not universally enhance but occasionally mitigate the toxic effects of PAHs [53].

In this study, although individual exposure to the two tested concentrations of PS-NPs showed no toxicity, a synergistic effect was observed when PS-NPs and PHE were combined, which increased at

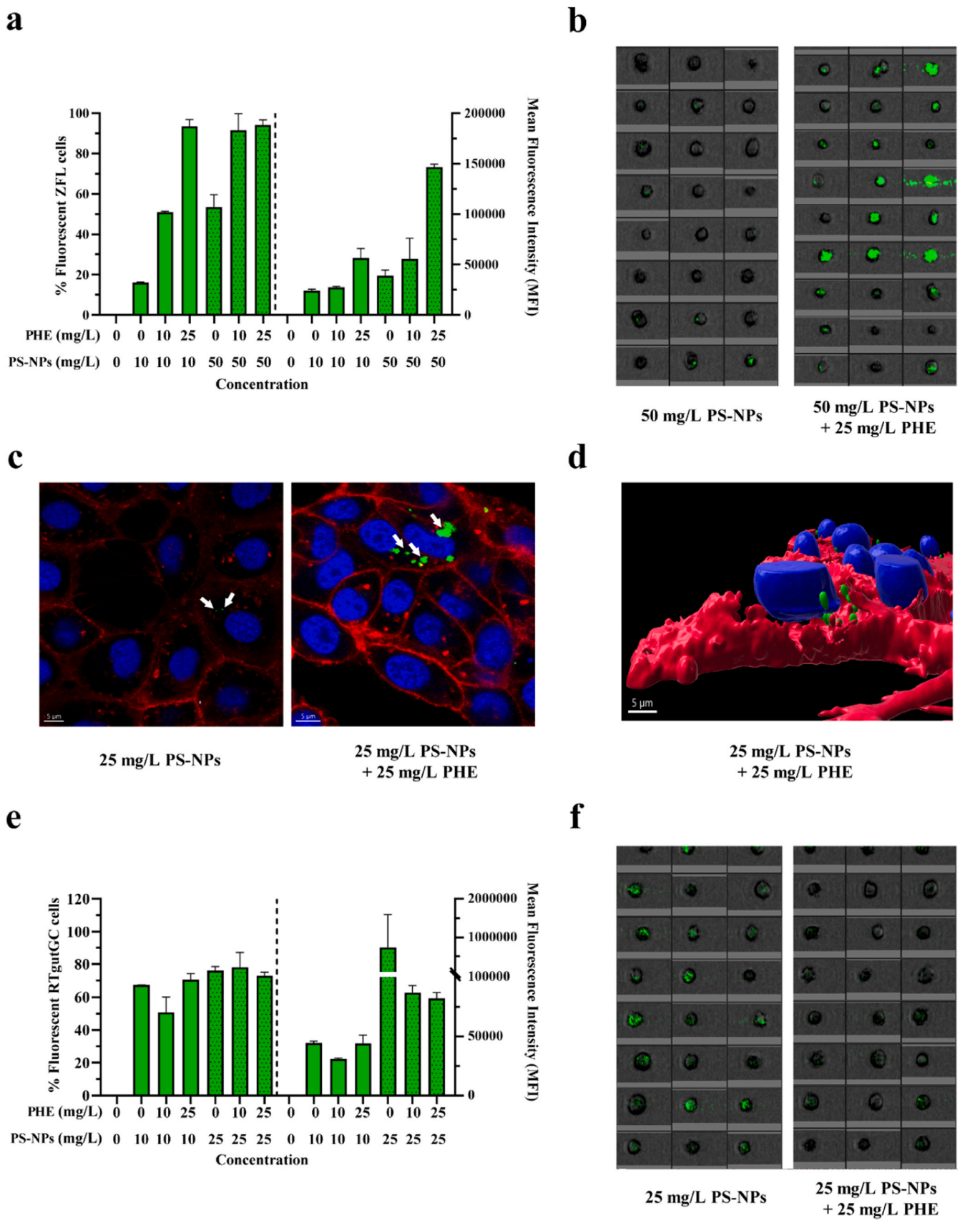

Fig. 2. (a, e): Uptake of fluorescently labelled PS-NPs by ZFL or RTgutGC cells. (a) Uptake in ZFL (e) Uptake in RTgutGC cells. (b, f): Individual images of ZFL (b) and RTgutGC (f) cells obtained from single exposure of PS-NPs versus co-exposure with PHE. (c, d): 2D (c) and 3D (d) confocal microscopy images of PS-NPs exposed individually or with PHE in ZFL cells. Green fluorescence corresponds to PS-NPs; blue and magenta to Hoechst-stained nuclei (N) and Cell Mask-stained plasma membrane, respectively.

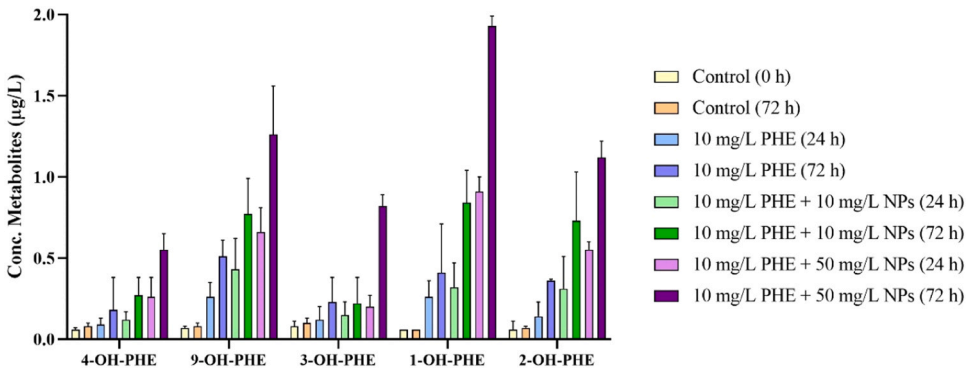

Fig. 3. Concentration of PHE metabolites when exposed to nominal 10 mg·L^{-1} PHE with or without 10 mg·L^{-1} or 50 mg·L^{-1} PS-NPs in ZFL cells at 24 h and 72 h. Significance levels *p < 0.05 (no significant data).

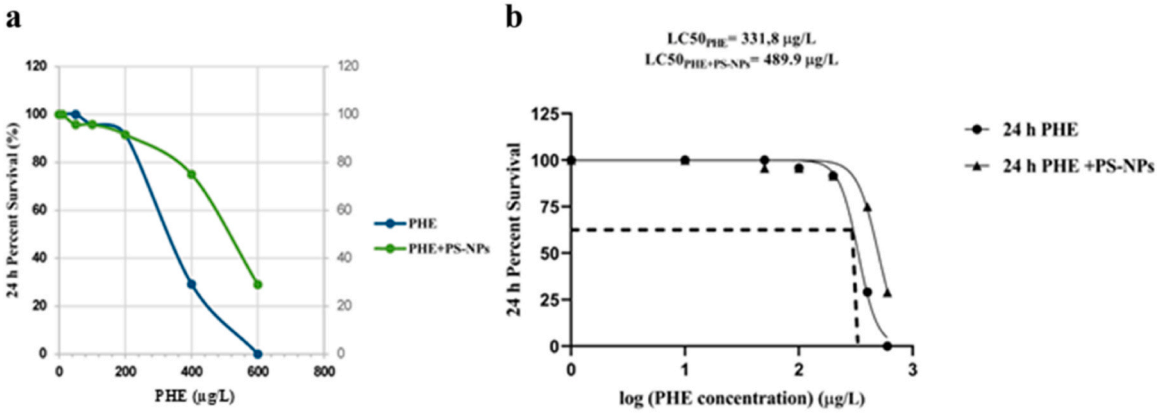

Fig. 4. (a) Survival of PHE treated zebrafish larvae or PHE plus PS-NPs (n = 24). (b) Probit analysis of LC_{50} values of PHE and PHE with 5 mg·L^{-1} PS-NPs at nominal concentrations on zebrafish larvae 24 h after exposure.

higher PS-NPs concentrations. This suggests a 'Trojan horse effect' where PS-NPs facilitate the PHE uptake, leading to higher toxicity. Nevertheless, PHE uptake results (Table 2), indicate that only RTgutGC cells showed higher accumulation of PHE (both in concentration and BCF value) when co-exposed with PS-NPs. When ZFL cells were exposed to PHE in combination with PS-NPs, lower concentrations of PHE and BCF were obtained, although they have a greater tendency than RTgutGC cells to accumulate PHE. Several studies [10,22,25], have reported higher PAH accumulation in single exposures compared to co-exposure with MNPs in different organisms. Narayanan *et al.* [14] analysed the zeta potential and hydrodynamic radius of NPs with and without PAHs, finding that PS-NPs adsorption of contaminants increased negative charges and hydrodynamic size. This suggests that PAH adsorption onto PS-NPs, may reduce PAH concentration in organisms such as microalgae. Another study, using molecular dynamics simulations examined PS-NPs and BaP uptake by dipalmitoylphosphatidylcholine (DPPC) bilayers. The findings showed that PS-NPs adsorb and accumulate BaP in water, facilitating its transport into the bilayer. Additionally, the adsorbed BaP enhanced PS-NP penetration into the DPPC bilayer through hydrophobic interactions [30]. The different functionalities and uptake dynamics of each cell type must be considered. Intestinal cells have a higher PS-NPs uptake capacity than ZFL as observed by flow cytometry and discussed below, however, this was not the case in the presence of PHE in the medium. Therefore, the higher concentration of PHE observed in RTgutGC cells in the presence of PS-NPs, compared to ZFL cells, cannot be attributed to an increased hydrodynamic radius that would prevent ZFL cells from internalizing PS-NPs with adsorbed PHE. Hepatocytes have an increased capacity to metabolise and detoxify xenobiotics and it is well known that aquatic organisms such as fish rapidly biotransform PAHs via cytochrome P450 (CYP1A) [54], playing a crucial role in reducing bioaccumulation [55]. In this study, higher concentrations of the major PHE metabolites were detected when ZFL cells were exposed to PHE in combination with higher concentrations of PS-NPs (Figure 3 and S4), which may explain the lower concentration of PHE found inside the cell. Rehman *et al.* [56] noted alterations in metabolic pathways when zebrafish were exposed to NPs and Li *et al.* [53] reported that co-exposure of MPs and PHE caused changes in metabolic profiles and pathways in zebrafish larvae. Martínez-Alvarez *et al.* [10] observed an increase in cyp1a (CYP450) levels in adult zebrafish when exposed to MPs but this did not occur when exposed in combination with BaP because it was too low concentration for effective bioaccumulation to activate biotransformation. Gene expression studies by Vazirzadeh *et al.* [57] also reported a clear association between the level of MPs and increased expression of liver enzymes such as glutathione S-transferase (GST) and CYP450, which are responsible for detoxifying pollutants such as PHE.

On the other hand, the focus has always been on the uptake of pollutants due to the presence of MNPs and few studies focus on the opposite effect. In this study, the uptake in ZFL cells increased in both cell number and intensity as there was a higher concentration of PHE in the medium (Fig. 2). This may be because free-form PHE caused damage to the cell membrane [58], allowing greater entry of PS-NPs. Another study measured the plasma membrane integrity of mussel hemocytes exposed to 50 nm PS-NPs and BaP and reported a significant descent of viability (membrane integrity) when exposed to the organic contaminant alone in comparison with the mixture with PS-NP [52]. This synergistic effect leads to a higher quantity of PS-NPs and a higher quantity of PHE attached to these PS-NPs, which we could observe in the case of

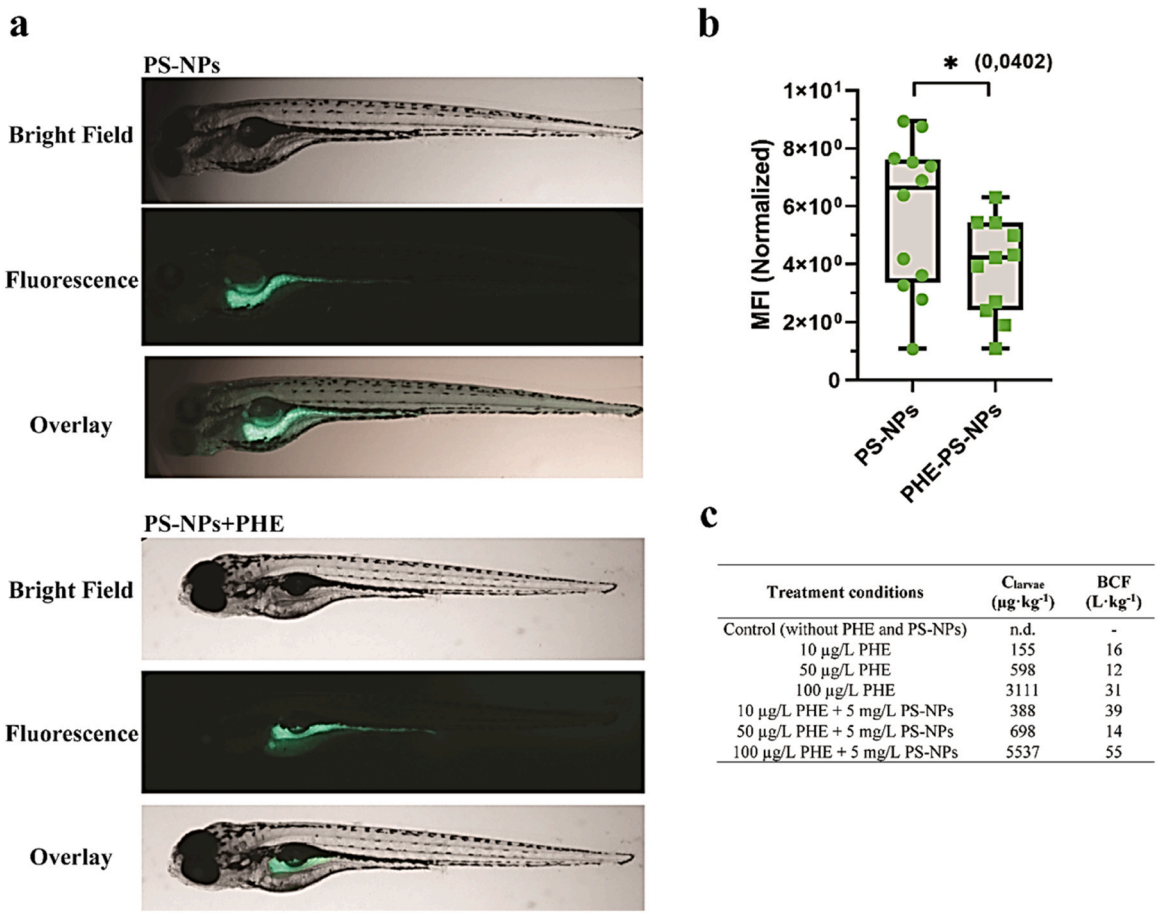

c

Treatment conditions	C_{larvae} (µg·kg^{-1})	BCF (L·kg^{-1})
Control (without PHE and PS-NPs)	n.d.	-
10 µg/L PHE	155	16
50 µg/L PHE	598	12
100 µg/L PHE	3111	31
10 µg/L PHE + 5 mg/L PS-NPs	388	39
50 µg/L PHE + 5 mg/L PS-NPs	698	14
100 µg/L PHE + 5 mg/L PS-NPs	5537	55

Fig. 5. Uptake of PS-NPs in the presence of PHE in zebrafish larvae. (a) Representative images of PS-NPs bioaccumulation. Animals were co-exposed to 5 mg/L of PS-NPs plus PHE for 48 h at 3 dpf. (b) Quantification of the Mean Fluorescence Intensity (MFI) in the zebrafish larvae. Bioaccumulation of PS-NPs was estimated at 5 dpf in the whole larvae. (c) PHE larvae concentration (C_{larvae}) and estimated BCF ($C_{larvae}/C_{exposure}$) 24 h after exposure. Images were analysed with ImageJ and the measured fluorescence was normalized to the larvae area. Statistical differences between treatments were analysed by unpair non-parametric Kolmogorov-Smirnov test Significance levels *$p < 0.05$. n.d.: not detected.

liver cells through the Trojan horse effect. However, the opposite effect was observed for RTgutGC cells, i.e. less PS-NPs in the presence of PHE, although RTgutGC cells have a greater tendency to uptake PS-NPs than ZFL cells. This may be due to the different functionalities and mechanisms of action and absorption of hepatocytes and enterocytes. ZFL cells are hepatocytes expressing specific xenobiotic membrane receptors such as the aryl hydrocarbon receptor (AhR), which plays an important role in the control of PAH metabolism [59], that may lead to a better entry of PS-NPs with PHE attached than in enterocytes. This difference of behavior between different types of cells has been also observed by Wang *et al.*, 2024 [32]. They found that hemocytes, a type of immune cells, exhibited higher sensitivity to pollutant-induced oxidative stress compared to the gills, which exhibit greater resistance to this type of stress. This difference in sensitivity may be attributed to the gills' lower metabolic activity or their reduced uptake of pollutants compared to hemocytes. Moreover, another important aspect is the internalization mechanism according to the cell type and size of the NPs [60,61]. Ramsperger *et al.* [62] suggested that active endocytosis plays a crucial role for larger plastic particles and that smaller particles are internalized by passive transport into cells. Zhang *et al.* [26] asserted that larger particles can be more easily enveloped by the cell membrane, however, it is a slower and more costly mechanism than passive transport. This difference may be attributed to the results obtained in this study, specifically that the lower internalization of PS-NPs was caused by an increase in size due to the adsorption of PHE on their surface [14].

4.2. Antagonistic and synergistic effects between PHE and PS-NPs in zebrafish larvae

In contrast to the findings in cell lines, zebrafish larvae exhibited decreased viability when PHE was exposed in combination with PS-NPs (Fig. 4). Since the concentrations of PS-NPs used in this work are not potentially toxic, the decrease in viability is due to the entry of PHE or to a synergic effect. Using fluorescent based-methodologies, we observed less internalization of PS-NPs in the presence of PHE (Fig. 5), possibly due to the increased hydrodynamic size of PS-NPs due to PHE adsorption, as demonstrated by Narayaman *et al.* [14], which could hinder their internalization. This might suggest that less PHE was internalized in larvae due to its adsorption to PS-NPs. However, a higher concentration of PHE was detected inside the larvae when PS-NPs were present in the medium (Fig. 5c). Therefore, although the observed increase in concentration is not very significant, and therefore not decisive to show an effect on toxicity, a 'Trojan horse effect' is being observed where the internalizing PS-NPs promote the entry of PHE. Ma *et al.* showed an additive effect on toxicity when co-exposing 50 nm NPs and phenanthrene in *Daphia magna* and the bioaccumulation of phenanthrene metabolites was significantly increased [63]. Xu *et al.* studied the internalisation of PHE (0.2 mg·L^{-1}) and PS-MPs (3 mg·L^{-1}) over time in adult zebrafish and observed a synergistic effect, increasing the bioaccumulation of both [64]. The same authors co-exposed PS-NPs (80 nm, 5 mg·L^{-1}) and PHE (0.1 mg·L^{-1}) and they also observed a more negative effect on zebrafish embryo morphology and mortality, but only

from the time the embryos opened their mouths [65].

In contrast to previous reports, we observed antagonistic effects on PS-NPs accumulation in the presence of PHE and on toxicity in the presence of PS-NPs, despite a synergistic effect on PHE accumulation. One potential factor influencing these outcomes is the different state of PHE in the two scenarios. Although the total concentration of PHE inside the larvae was higher in the presence of PS-NPs, the free concentration of PHE was lower both in the medium and in the larvae [25]. This free concentration may be the primary cause of the observed toxic effect. Furthermore, free PHE enters faster and easier by passive diffusion [66] compared to the PHE adsorbed by PS-NPs, as observed in fluorescence. Other studies in literature also report antagonistic effects. Trevisan *et al.* [25] suggested that exposure to NPs together with mixed PAHs could activate defence mechanisms that reduce toxicity. Similarly, other studies have reported an antagonistic effect on toxicity [53] and a "cleaning effect" where cleaner or less contaminated MNPs can mitigate the effects of POPs [67,68].

5. Conclusions

The interaction between PS-NPs and PHE is highly complex, with ecotoxicological effects varying across cell and tissue type. Our data show that the combined presence of PS-NPs and PHE induces distinct cellular responses which widely differ across biological systems. These effects include differences in uptake, metabolic activity and toxicity response. The lower uptake of PS-NPs in the presence of PHE in intestinal cells and zebrafish larvae, contrasting with higher uptake in liver cells, suggests a tissue-specific uptake mechanism of these co-pollutants. Moreover, the lower toxicity of PHE in the presence of PS-NPs in zebrafish larvae raises the possibility that PS-NPs may modulate the bioavailability and thus toxicity of organic pollutants. The high levels of PHE metabolites detected in liver cells further indicate that PS-NPs may alter the xenobiotics metabolism, which could have significant implications for bioaccumulation and long-term toxicity in living organisms.

We hypothesize that NPs can adsorb contaminants, potentially reducing their uptake due to particle agglomeration. This underscores the necessity to consider the combined effects of multiple contaminants in ecological risk assessments, as single contaminant studies may underestimate the hazards posed by complex environmental mixtures. Furthermore, the differential cellular and tissue responses to PS-NPs and PHE exposure highlight the need for targeted research to better understand the mechanisms driving these interactions. Our findings provide an important basis for future investigation aimed at elucidating the long-term ecological consequences of co-pollutant interaction.

Environmental implications

Nanoplastics have a significant environmental impact, but they rarely occur isolated; they interact with coexisting pollutants, which can amplify ecological and toxicological effects. Some studies have already shown that nanoplastics act as carriers of toxic compounds, but contradictions remain about their effects and mechanisms of action remain unclear. This work examines co-exposure using different aquatic models to analyze organ- and organism-specific impacts. The goal is to better understand their behavior in the environment and provide information for developing more effective strategies to protect human health, organisms, and ecosystems and its long-term consequences.

CRediT authorship contribution statement

Jon Sanz-Landaluze: Writing – review & editing, Visualization, Validation, Supervision, Software, Resources, Project administration, Methodology, Funding acquisition, Data curation, Conceptualization. **Nerea Roher:** Writing – review & editing, Visualization, Validation, Supervision, Software, Resources, Project administration, Methodology, Funding acquisition, Data curation, Conceptualization. **Marlid Garcia-Ordoñez:** Writing – original draft, Validation, Supervision, Software, Methodology, Investigation, Formal analysis, Data curation. **Paloma De Oro-Carretero:** Writing – original draft, Visualization, Validation, Supervision, Software, Methodology, Investigation, Formal analysis, Data curation.

Declaration of Competing Interest

The authors declare that they have no known competing financial interests or personal relationships that could have appeared to influence the work reported in this paper.

Acknowledgments

The present study was supported by the Spanish Ministry of Science and Innovation [PID2023–148425NB-I00] to JSL and PID2021–126710OB-C21 MINECO/FEDER and 2021-SGR-00068 AGAUR to NR. The authors thank Dr. C. Tafalla's laboratory for providing RTGutGC cells [44]. Paloma de Oro and Marlid Garcia thank the Spanish Ministry of Science and Innovation for their predoctoral contract [PRE2021/097956; PRE2022–103797, respectively].

Appendix A. Supporting information

Supplementary data associated with this article can be found in the online version at doi:10.1016/j.jhazmat.2025.139356.

Data availability

No data was used for the research described in the article.

References

[1] Kushwaha, M., Shankar, S., Goel, D., Singh, S., Rahul, J., Rachna, K., Singh, J., 2024. Microplastics pollution in the marine environment: a review of sources, impacts and mitigation. Mar Pollut Bull 209. https://doi.org/10.1016/j.marpolbul.2024.117109.

[2] Bidashimwa, D., Hoke, T., Huynh, T.B., Narkpitaks, N., Priyonugroho, K., Ha, T.T., Burns, A., Weissman, A., 2023. Plastic pollution: How can the global health community fight the growing problem? BMJ Glob Health 8. https://doi.org/10.1136/bmjgh-2023-012140.

[3] Prokić, M.D., Gavrilović, B.R., Radovanović, T.B., Gavrić, J.P., Petrović, T.G., Despotović, S.G., Faggio, C., 2021. Studying microplastics: lessons from evaluated literature on animal model organisms and experimental approaches. J Hazard Mater 414. https://doi.org/10.1016/j.jhazmat.2021.125476.

[4] Waller, C.L., Griffiths, H.J., Waluda, C.M., Thorpe, S.E., Loaiza, I., Moreno, B., Pacherres, C.O., Hughes, K.A., 2017. Microplastics in the Antarctic marine system: An emerging area of research. Sci Total Environ 598, 220–227. https://doi.org/10.1016/j.scitotenv.2017.03.283.

[5] Materić, D., Peacock, M., Dean, J., Futter, M., Maximov, T., Moldan, F., Röckmann, T., Holzinger, R., 2022. Presence of nanoplastics in rural and remote surface waters. Environ Res Lett 17. https://doi.org/10.1088/1748-9326/ac68f7.

[6] Vitali, C., Peters, R.J.B., Janssen, H.G., Nielen, M.W.F., 2023. Microplastics and nanoplastics in food, water, and beverages; part I. occurrence. TrAC Trends Anal Chem 159. https://doi.org/10.1016/j.trac.2022.116670.

[7] Al-Thawadi, S., 2020. Microplastics and Nanoplastics in Aquatic Environments: Challenges and Threats to Aquatic Organisms. Arab J Sci Eng 45, 4419–4440. https://doi.org/10.1007/s13369-020-04402-z.

[8] Kik, K., Bukowska, B., Sicińska, P., 2020. Polystyrene nanoparticles: Sources, occurrence in the environment, distribution in tissues, accumulation and toxicity to various organisms. Environ Pollut 262. https://doi.org/10.1016/j.envpol.2020.114297.

[9] Erni-Cassola, G., Zadjelovic, V., Gibson, M.I., Christie-Oleza, J.A., 2019. Distribution of plastic polymer types in the marine environment; a meta-analysis. J Hazard Mater 369, 691–698. https://doi.org/10.1016/j.jhazmat.2019.02.067.

[10] Martínez-Álvarez, I., Le Menach, K., Cajaraville, M.P., Budzinski, H., Orbea, A., 2024. Effects of polystyrene nano- and microplastics and of microplastics with sorbed polycyclic aromatic hydrocarbons in adult zebrafish. Sci Total Environ 927. https://doi.org/10.1016/j.scitotenv.2024.172380.

[11] Jambeck, J.R., Geyer, R., Wilcox, C., Siegler, T.R., Perryman, M., Andrady, A., Narayan, R., Law, K.L., 2015. Plastic waste inputs from land into the ocean. Science 347 (1979), 768–771. https://doi.org/10.1126/science.1260352.

[12] Patidar, K., Alshehri, M., Singha, W., Alrasheedi, M., Younis, A.M., Dumka, U.C., Ambade, B., 2025. Assessing the microplastic pandemic: prevalence, detection, and human health impacts in Asian aquatic environments. Phys Chem Earth 137. https://doi.org/10.1016/j.pce.2024.103800.

[13] M. Bergmann, L. Gutow, M. Klages, Marine Anthropogenic Litter, n.d.
[14] Narayanan, G., Talib, M., Singh, N., Darbha, G.K., 2024. Toxic effects of polystyrene nanoplastics and polycyclic aromatic hydrocarbons (chrysene and fluoranthene) on the growth and physiological characteristics of Chlamydomonas reinhardtii. Aquat Toxicol 268. https://doi.org/10.1016/j.aquatox.2024.106838.
[15] Dai, J., Song, B., Sha, R., Wang, Z., Mao, J., 2025. The effects of single and combined exposure to polystyrene nanoplastics and copper on the behavior of adult zebrafish. Water (Switzerland) 17. https://doi.org/10.3390/w17030392.
[16] Gallego-Urrea, J.A., Tuoriniemi, J., Pallander, T., Hassellöv, M., 2010. Measurements of nanoparticle number concentrations and size distributions in contrasting aquatic environments using nanoparticle tracking analysis. Environ Chem 7, 67–81. https://doi.org/10.1071/EN09114.
[17] Materić, D., Kasper-Giebl, A., Kau, D., Anten, M., Greilinger, M., Ludewig, E., Van Sebille, E., Röckmann, T., Holzinger, R., 2020. Micro-and nanoplastics in alpine snow: a new method for chemical identification and (semi)quantification in the nanogram range. Environ Sci Technol 54, 2353–2359. https://doi.org/10.1021/acs.est.9b07540.
[18] Pabortsava, K., Lampitt, R.S., 2020. High concentrations of plastic hidden beneath the surface of the Atlantic Ocean. Nat Commun 11. https://doi.org/10.1038/s41467-020-17932-9.
[19] Chang, L., Bai, S., Wei, P., Gao, X., Dong, J., Zhou, B., Peng, C., Jia, J., Luan, T., 2024. Quantitative detecting low concentration polystyrene nanoplastics in aquatic environments via an Ag/Nb2CTx (MXene) SERS substrate. Talanta 273. https://doi.org/10.1016/j.talanta.2024.125859.
[20] Shi, C., Liu, Z., Yu, B., Zhang, Y., Yang, H., Han, Y., Wang, B., Liu, Z., Zhang, H., 2024. Emergence of nanoplastics in the aquatic environment and possible impacts on aquatic organisms. Sci Total Environ 906. https://doi.org/10.1016/j.scitotenv.2023.167404.
[21] Yee, M.S.L., Hii, L.W., Looi, C.K., Lim, W.M., Wong, S.F., Kok, Y.Y., Tan, B.K., Wong, C.Y., Leong, C.O., 2021. Impact of microplastics and nanoplastics on human health. Nanomaterials 11, 1–23. https://doi.org/10.3390/nano11020496.
[22] Stapleton, P.A., 2019. Toxicological considerations of nano-sized plastics. AIMS Environ Sci 6, 367–378. https://doi.org/10.3934/environsci.2019.5.367.
[23] Brandts, I., Garcia-Ordoñez, M., Tort, L., Teles, M., Roher, N., 2020. Polystyrene nanoplastics accumulate in ZFL cell lysosomes and in zebrafish larvae after acute exposure, inducing a synergistic immune response: In vitro without affecting larval survival in vivo. Environ Sci Nano 7, 2410–2422. https://doi.org/10.1039/d0en00553c.
[24] Hu, Y., Nie, F., Zhang, M., Song, Q., Wei, W., Lv, G., Wei, Y., Kang, D., Chen, Z., Lin, H., Chen, J., 2024. Developmental toxicity and mechanism of polychlorinated biphenyls 126 and nano-polystyrene combined exposure to zebrafish larvae. Ecotoxicol Environ Saf 278. https://doi.org/10.1016/j.ecoenv.2024.116419.
[25] Trevisan, R., Voy, C., Chen, S., Di Giulio, R.T., 2019. Nanoplastics decrease the toxicity of a complex PAH mixture but impair mitochondrial energy production in developing Zebrafish. Environ Sci Technol 53, 8405–8415. https://doi.org/10.1021/acs.est.9b02003.
[26] Zhang, Y., Goss, G.G., Goss, G.G., Goss, G.G., 2020. Potentiation of polycyclic aromatic hydrocarbon uptake in zebrafish embryos by nanoplastics. Environ Sci Nano 7, 1730–1741. https://doi.org/10.1039/d0en00163e.
[27] Liu, L., Fokkink, R., Koelmans, A.A., 2016. Sorption of polycyclic aromatic hydrocarbons to polystyrene nanoplastic. Environ Toxicol Chem 35, 1650–1655. https://doi.org/10.1002/etc.3311.
[28] Arikan, B., Ozfidan-Konakci, C., Yildiztugay, E., Turan, M., Cavusoglu, H., 2022. Polystyrene nanoplastic contamination mixed with polycyclic aromatic hydrocarbons: alleviation on gas exchange, water management, chlorophyll fluorescence and antioxidant capacity in wheat. Environ Pollut 311. https://doi.org/10.1016/j.envpol.2022.119851.
[29] Yu, H., Yang, B., Waigi, M.G., Peng, F., Li, Z., Hu, X., 2020. The effects of functional groups on the sorption of naphthalene on microplastics. Chemosphere 261. https://doi.org/10.1016/j.chemosphere.2020.127592.
[30] Cheng, S., Ye, Z., Wang, X., Lian, C., Shang, Y., Liu, H., 2023. The effects of adsorbed benzo(a)pyrene on dynamic behavior of polystyrene nanoplastics through phospholipid membrane: a molecular simulation study. Colloids Surf B Biointerfaces 224. https://doi.org/10.1016/j.colsurfb.2023.113211.
[31] Marvin, C.H., Tomy, G.T., Thomas, P.J., Holloway, A.C., Sandau, C.D., Idowu, I., Xia, Z., 2020. Considerations for prioritization of polycyclic aromatic compounds as environmental contaminants. Environ Sci Technol 54, 14787–14789. https://doi.org/10.1021/acs.est.0c04892.
[32] Wang, S., Ma, L., Chen, L., Sokolova, I.M., Huang, W., Li, D., Hu, M., Khan, F.U., Shang, Y., Wang, Y., 2024. The combined effects of phenanthrene and micro-/nanoplastics mixtures on the cellular stress responses of the thick-shell mussel Mytilus coruscus. Environ Pollut 341. https://doi.org/10.1016/j.envpol.2023.122999.
[33] Liu, B., Gao, L., Ding, L., Lv, L., Yu, Y., 2023. Trophodynamics and bioaccumulation of polycyclic aromatic hydrocarbons (PAHs) in marine food web from Laizhou Bay, China. Mar Pollut Bull 194. https://doi.org/10.1016/j.marpolbul.2023.115307.
[34] Xu, K., Ai, W., Wang, Q., Tian, L., Liu, D., Zhuang, Z., Wang, J., 2022. Toxicological effects of nanoplastics and phenanthrene to zebrafish (Danio rerio). Gondwana Res 108, 127–132. https://doi.org/10.1016/j.gr.2021.05.012.
[35] Peng, X., Sun, X., Yu, M., Fu, W., Chen, H., Chen, J., 2019. Chronic exposure to environmental concentrations of phenanthrene impairs zebrafish reproduction. Ecotoxicol Environ Saf 182. https://doi.org/10.1016/j.ecoenv.2019.109376.
[36] Wu, J., Liu, Z., Yan, Z., Yi, X., 2015. Derivation of water quality criteria of phenanthrene using interspecies correlation estimation models for aquatic life in China. Environ Sci Pollut Res 22, 9457–9463. https://doi.org/10.1007/s11356-015-4091-9.
[37] Miura, K., Shimada, K., Sugiyama, T., Sato, K., Takami, A., Chan, C.K., Kim, I.S., Kim, Y.P., Lin, N.H., Hatakeyama, S., 2019. Seasonal and annual changes in PAH concentrations in a remote site in the Pacific Ocean. Sci Rep 9. https://doi.org/10.1038/s41598-019-47409-9.
[38] Bhagat, J., Zang, L., Nishimura, N., Shimada, Y., 2020. Zebrafish: an emerging model to study microplastic and nanoplastic toxicity. Sci Total Environ 728. https://doi.org/10.1016/j.scitotenv.2020.138707.
[39] Brandts, I., Solà, R., Garcia-Ordoñez, M., Gella, A., Quintana, A., Martin, B., Esteve-Codina, A., Teles, M., Roher, N., 2023. Polystyrene nanoplastics target lysosomes interfering with lipid metabolism through the PPAR system and affecting macrophage functionalization. Environ Sci Nano 10, 2245–2258. https://doi.org/10.1039/d2en01077a.
[40] Sendra, M., Pereiro, P., Yeste, M.P., Mercado, L., Figueras, A., Novoa, B., 2021. Size matters: Zebrafish (Danio rerio) as a model to study toxicity of nanoplastics from cells to the whole organism. Environ Pollut 268. https://doi.org/10.1016/j.envpol.2020.115769.
[41] Kramer, N.I., Krismartina, M., Rico-Rico, Á., Blaauboer, B.J., Hermens, J.L.M., 2012. Quantifying processes determining the free concentration of phenanthrene in basal cytotoxicity assays. Chem Res Toxicol 25, 436–445. https://doi.org/10.1021/tx200479k.
[42] Wang, J., Liu, X., Liu, G., Zhang, Z., Wu, H., Cui, B., Bai, J., Zhang, W., 2019. Size effect of polystyrene microplastics on sorption of phenanthrene and nitrobenzene. Ecotoxicol Environ Saf 173, 331–338. https://doi.org/10.1016/j.ecoenv.2019.02.037.
[43] Torrealba, D., Parra, D., Seras-Franzoso, J., Vallejos-Vidal, E., Yero, D., Gibert, I., Villaverde, A., Garcia-Fruitós, E., Roher, N., 2016. Nanostructured recombinant cytokines: a highly stable alternative to short-lived prophylactics. Biomaterials 107, 102–114. https://doi.org/10.1016/j.biomaterials.2016.08.043.
[44] Kawano, A., Haiduk, C., Schirmer, K., Hanner, R., Lee, L.E.J., Dixon, B., Bols, N.C., 2011. Development of a rainbow trout intestinal epithelial cell line and its response to lipopolysaccharide. Aquac Nutr 17. https://doi.org/10.1111/j.1365-2095.2010.00757.x.
[45] Morgan, A., Babu, D., Reiz, B., Whittal, R., Suh, L.Y.K., Siraki, A.G., 2019. Caution for the routine use of phenol red – It is more than just a pH indicator. Chem Biol Inter 310. https://doi.org/10.1016/j.cbi.2019.108739.
[46] Kuncharoenwirat, Nathaphon, Chatuphonprasert, Waranya, Jarukamjorn, Kanokwan, 2021. Effect of phenol red on cell cultures. IJPS 17, 13–23.
[47] De Oro-Carretero, P., Sanz-Landaluze, J., 2023. Miniaturized method for the quantification of persistent organic pollutants and their metabolites in HepG2 cells: assessment of their biotransformation. Anal Bioanal Chem 415, 4813–4825. https://doi.org/10.1007/s00216-023-04781-w.
[48] De Oro-Carretero, P., Sanz-Landaluze, J., 2024. In vitro approach to refine bioconcentration and biotransformation predictions of organic persistent pollutants using cell lines. Chemosphere 364. https://doi.org/10.1016/j.chemosphere.2024.143020.
[49] De Oro-Carretero, P., Sanz-Landaluze, J., 2023. Bioaccumulation and Biotransformation of BDE-47 Using Zebrafish Eleutheroembryos (Danio rerio). Environ Toxicol Chem 42, 835–845. https://doi.org/10.1002/etc.5569.
[50] Sun, N., Wang, J., Shi, H., Li, X., Guo, S., Wang, Y., Hu, S., Liu, R., Gao, C., 2023. Compound effect and mechanism of oxidative damage induced by nanoplastics and benzo [a] pyrene. J Hazard Mater 460. https://doi.org/10.1016/j.jhazmat.2023.132513.
[51] Trevisan, R., Uzochukwu, D., Di Giulio, R.T., 2020. PAH Sorption to Nanoplastics and the Trojan Horse Effect as Drivers of Mitochondrial Toxicity and PAH Localization in Zebrafish. Front Environ Sci 8. https://doi.org/10.3389/fenvs.2020.00078.
[52] Katsumiti, A., Losada-Carrillo, M.P., Barros, M., Cajaraville, M.P., 2021. Polystyrene nanoplastics and microplastics can act as Trojan horse carriers of benzo(a)pyrene to mussel hemocytes in vitro. Sci Rep 11. https://doi.org/10.1038/s41598-021-01938-4.
[53] Li, J., Liu, X., Fu, J., Gong, Z., Jiang, S.Y., Chen, J.P., 2024. Metabolic profile changes of zebrafish larvae in the single- and co-exposures of microplastics and phenanthrene. Sci Total Environ 953. https://doi.org/10.1016/j.scitotenv.2024.175994.
[54] D.R. Livingstone, The fate of organic xenobiotics in aquatic ecosystems: quantitative and qualitative differences in biotransformation by invertebrates and fish, 1998.
[55] Fu, Q., Fedrizzi, D., Kosfeld, V., Schlechtriem, C., Ganz, V., Derrer, S., Rentsch, D., Hollender, J., 2020. Biotransformation changes bioaccumulation and toxicity of diclofenac in aquatic organisms. Environ Sci Technol 54, 4400–4408. https://doi.org/10.1021/acs.est.9b07127.
[56] Rehman, A., Huang, F., Zhang, Z., Habumugisha, T., Yan, C., Shaheen, U., Zhang, X., 2024. Nanoplastic contamination: Impact on zebrafish liver metabolism and implications for aquatic environmental health. Environ Int 187. https://doi.org/10.1016/j.envint.2024.108713.
[57] Vazirzadeh, A., Ergun, S., Mossafa, H., Farhadi, A., Keshavarzifard, M., Yigit, M., Yilmaz, S., 2025. Microplastics contamination suppressed immune and health status in cage cultured Barramundi: an investigation on pollution sources, ecotoxicological impacts, and transcription of genes involved in detoxification. Aquaculture 594. https://doi.org/10.1016/j.aquaculture.2024.741370.
[58] He, F., Hu, S., Liu, R., Li, X., Guo, S., Wang, H., Tian, G., Qi, Y., Wang, T., 2023. Decoding the biological toxicity of phenanthrene on intestinal cells of Eisenia

fetida: Effects, toxicity pathways and corresponding mechanisms. Sci Total Environ 904. https://doi.org/10.1016/j.scitotenv.2023.166903.
[59] Vondráček, J., Machala, M., 2020. The role of metabolism in toxicity of polycyclic aromatic hydrocarbons and their non-genotoxic modes of action. Curr Drug Metab 22, 584–595. https://doi.org/10.2174/1389200221999201125205725.
[60] Hou, Z., Meng, R., Chen, G., Lai, T., Qing, R., Hao, S., Deng, J., Wang, B., 2022. Distinct accumulation of nanoplastics in human intestinal organoids. Sci Total Environ 838. https://doi.org/10.1016/j.scitotenv.2022.155811.
[61] Geum, S.W., Yeo, M.K., 2022. Reduction in toxicity of polystyrene nanoplastics combined with phenanthrene through binding of jellyfish mucin with nanoplastics. Nanomaterials 12. https://doi.org/10.3390/nano12091427.
[62] A.F.R.M. Ramsperger, V.K.B. Narayana, W. Gross, J. Mohanraj, M. Thelakkat, A. Greiner, H. Schmalz, H. Kress, C. Laforsch, Environmental exposure enhances the internalization of microplastic particles into cells, 2020.
[63] Ma, Y., Huang, A., Cao, S., Sun, F., Wang, L., Guo, H., Ji, R., 2016. Effects of nanoplastics and microplastics on toxicity, bioaccumulation, and environmental fate of phenanthrene in fresh water. Environ Pollut 219, 166–173. https://doi.org/10.1016/j.envpol.2016.10.061.
[64] Xu, K., Zhang, Y., Huang, Y., Wang, J., 2021. Toxicological effects of microplastics and phenanthrene to zebrafish (Danio rerio). Sci Total Environ 757. https://doi.org/10.1016/j.scitotenv.2020.143730.
[65] Xu, K., Ai, W., Wang, Q., Tian, L., Liu, D., Zhuang, Z., Wang, J., 2022. Toxicological effects of nanoplastics and phenanthrene to zebrafish (Danio rerio). Gondwana Res 108, 127–132. https://doi.org/10.1016/j.gr.2021.05.012.
[66] Stott, L.C., Schnell, S., Hogstrand, C., Owen, S.F., Bury, N.R., 2015. A primary fish gill cell culture model to assess pharmaceutical uptake and efflux: evidence for passive and facilitated transport. Aquat Toxicol 159, 127–137. https://doi.org/10.1016/j.aquatox.2014.12.007.
[67] Zhang, M., Xu, L., 2022. Transport of micro- and nanoplastics in the environment: Trojan-Horse effect for organic contaminants. Crit Rev Environ Sci Technol 52, 810–846. https://doi.org/10.1080/10643389.2020.1845531.
[68] Koelmans, A.A., Besseling, E., Wegner, A., Foekema, E.M., 2013. Plastic as a carrier of POPs to aquatic organisms: a model analysis. Environ Sci Technol 47, 7812–7820. https://doi.org/10.1021/es401169n.